Paper:

Paunovi, S., Caji, M., Karlii, D. & Mijalkovi, M. (2019). A novel approach for vibration analysis of fractional viscoelastic beams with attached masses and base excitation. *Journal of Sound and Vibration, 463*, 114955

http://dx.doi.org/10.1016/j.jsv.2019.114955

A novel approach for vibration analysis of fractional viscoelastic beams with attached masses and base excitation

Stepa Paunović [a], Milan Cajić [a,*], Danilo Karličić [a,b], Marina Mijalković [c]

[a] Mathematical institute of the Serbian Academy of Sciences and Arts, Kneza Mihaila 36, Belgrade, Serbia
[b] College of Engineering, Swansea University, United Kingdom
[c] Faculty of Civil Engineering and Architecture, University of Niš, Aleksandra Medvedeva 14, Niš, Serbia

Abstract

The Galerkin method is widely applied for finding approximate solutions to vibration problems of beam and plate structures and for estimating their dynamic behaviour. Most studies employ the Galerkin method in the analysis of the undamped systems, or for simple structure models with viscous damping. In this paper, a novel approach of using the Galerkin method and Fourier transform to find the solution to the problem of vibration of fractionally damped beams with an arbitrary number of attached concentrated masses and base excitation is presented. The considered approach is novel and it lends itself to determination of the impulse response of the beam and leads to the solution of the system of coupled fractional order differential equations. The proposed approximate solution is validated against the exact solution for a special case with only one tip mass attached, as well as against the Finite Element Method Solution for a special case with classical viscous damping model. Numerical analysis is also given, including the examples of vibration analysis of viscoelastic beams with different fractional derivative orders, retardation times, and the number, weight and position of the attached masses.

Keywords: Galerkin method, fractional viscoelasticity, beam mass system, base excitation, impulse response

1. Introduction

Many mechanical systems commonly met in practice can be modelled as a cantilever beam with one or more attached concentrated masses. Application of such systems ranges from civil engineering [1] to mechanical engineering [2]

*Corresponding author
Email address: mcajic@mi.sanu.ac.rs (Milan Cajić)

purposes and they have been addressed in experimental and theoretical studies extensively over the last several decades. Most of the first approaches to treat such systems were based on analytical techniques to reach exact frequency equations, eigenvalues and the corresponding eigenfunctions. One of the first approaches to find the exact frequencies and mode shape functions, for a beam with attached mass introduced via Dirac delta function, was based on spatial domain Laplace transform method [3]. The cited author has solved the initial value and forced vibration problems by using eigenfunctions orthogonal with respect to a new weighting function. Another commonly used method to obtain the exact eigenfrequency equation and mode shapes is based on compatibility conditions introduced at the place of the attached mass. In [4], this method has been compared to the method based on Laplace transform, where it was confirmed that both methods yield exactly the same eigenvalues. Analytic form of frequency equations can be obtained, but it has been shown to be a comprehensive task with the increase of the number of concentrated masses. In addition, some authors have used the generalised functions to deal with beams with internal discontinuities such as changes in stiffness and/or material properties, and external discontinuities in the form of attached elements or additional boundary conditions [5, 6] .

Another approach for obtaining the solution for the beam mass problem is based on approximate methods such as Rayleigh-Ritz or Galerkin method [7]. Such methods are much easier to apply to problems with multiple attached masses since they do not demand derivation of orthogonality relations or calculation of complex frequency equations. Hamdan and Latif [8] solved the beam mass problem using approximate methods and compared them to the exact and numerical solution based on the finite element method. The authors have compared the numerical results to the exact solution, and it was shown that the finite element method yielded the best approximation, while the Galerkin method results significantly improve by increasing the number of considered modes. In that paper, it was also confirmed that Rayleigh-Ritz method was computationally less expensive than the Galerkin method but it yielded a larger error. In the literature, there are also analytical-and-numerical-combined methods (ANCM) [9, 10] that are suitable for the problems of beams carrying concentrated masses or spring-damper-mass systems. In comparison to transfer matrix and finite element methods, it was demonstrated that such combined methods could be more efficient and even faster than the finite element method but at the expense of accuracy of the results. Recently, much effort has been devoted to experimental and theoretical investigation of nanotube based mass detection sensors. Non-atomic based theories to model nanotubes as nanobeam structures mostly relies on modified continuum theories to account for the small scale effects. This results in complex governing equations for the vibration of nanobeams with concentrated masses representing nanoparticles at the molecular level. However, such models are much simpler and computationally more efficient compared to the atomistic ones. Solution methods for nanobeam mass problems are similar to the classical ones and range from application of the finite element method [11], differential quadrature method [12], Galerkin method [13], and transfer function method [14] to meshless techniques [15, 16].

Consideration of structural damping in beam vibration problems is important step in achieving a more accurate response. Depending on the source of dissipation, damping can be divided into two main categories, the external and internal damping. The former are usually described by using some of the available models of viscoelastic body, while the external damping is usually considered as viscous type of damping [17]. Further, classical viscoelastic or viscous damping constitutive relations can be divided into differential and integral type of models. Using the aforementioned relations in structural vibration analysis leads to damped vibration problems, where governing equations after spatial discretization become time dependent differential equations with the corresponding stiffness, mass and damping matrices and the corresponding eigenvalue problem with complex frequencies [18, 19]. Nevertheless, the fractional order derivative viscoelastic models are shown to be advantageous compared to the classical integer order ones, since they require fewer parameters in order to fit experimental data [20]. History of fractional rheological models dates back to Scott Blair and Gerasimov and later they were applied by many authors to describe the materials with behavior ranging from fluid like to solid like behavior [21]. Rossikhin and Shitikova [22] reviewed a large amount of literature concerning the application of fractional calculus to various dynamic problems in solid mechanics. Problems of vibration of fractional viscoelastic beam and rod structure based models were studied in numerous papers [23]. [23, 24] studied the longitudinal and transverse vibrations of rod and beam structures using fractional order derivative constitutive equations. The problems were solved using the corresponding eigenvalue problem and power series solution. Atanackovic et al. [25] performed a comprehensive study on different problems in mechanics described via fractional calculus based models. In spite that there is a vast literature on vibration of fractional viscoelastic structures [26–34] , only a few papers are considering such problems with concentrated masses, e.g. [35, 36]. Cajic et al. [37] analyzed the free transverse vibration of a nanobeam with a single attached mass using modified nonlocal and fractional viscoelastic constitutive equation. The authors used compatibility conditions to introduce the attached mass into the model and found the exact solution of the problem. In [38], the authors considered a more complex nonlocal fractional viscoelastic nanobeam model with an arbitrary number of attached masses and influence of the axial magnetic field and fractional viscoelastic foundation. In this case, however, an approximate solution for the free vibration problem was found.

The base excitation of beams is another interesting problem for analysis due to recent application for energy harvesting purposes [39]. The literature on this problem is sparse and some of the papers are considering elastic [40] and fractional viscoelastic beam models [41, 42]. Freundlich [43] analyzed the vibration of the fractional Kelvin-Voigt cantilever beam with base excitation and tip mass at the free end. The author used the separation of variables method and found the exact eigenvalues and eigenfunctions of the problem. After the derivation of the corresponding orthogonality relationship for eigenfunctions, a fractional differential equation is obtained and solved using the methodology from [44] based on impulse response and Green function as well as residue theory. The exact analytical solution obtained in this way is limited to problems with a single attached mass introduced through boundary conditions.

The aim of this study is to construct a more general model and solution method for the vibration of fractional viscoelastic beams with base excitation and an arbitrary number of concentrated masses attached to the beam. This is achieved by using the Galerkin method for space discretization, where the obtained system of coupled fractional order differential equations is solved using the methodology adopted from [44]. The presented approach is a step forward in investigation of this type of problems. The obtained solution is validated for a special case against the exact solution from [43] and numerical finite element method. The observed theoretical problem and the developed solution methods possess good potential for future use in energy harvesting devices with fractional damping considered. The developed methodology could be extended to consider the systems of multiple coupled beams with attached masses and base excitation for possible application as energy harvesting devices implemented in civil engineering structures and for green energy production.

2. Theoretical preliminaries

2.1. Fractional derivatives

If the order of a derivative is not an integer, but rather a real number, the derivative is called a fractional order derivative or simply *fractional derivative*. Derivatives of this kind are defined in fractional calculus, and they have already been used in various problems of mechanics [25]. Several definitions of fractional derivatives are in use. In this paper, the Riemann-Liouville definition is used, which can be stated as follows [45].

Let $\mathbb{N}$ and $\mathbb{C}$ denote the set of natural, and the set of complex numbers, respectively, and let $AC([a,b])$ denote the space of absolutely continuous functions, and $AC^n, n \in \mathbb{N}, n \geq 2$ denote the space of functions f that have continuous derivatives up to the order of $n-1$ and $f^{(n-1)} \in AC([a,b])$.

Definition 1. Let $\alpha \in \mathbb{C}, Re \quad \alpha \geq 0, n-1 < Re, \alpha < n, n \in \mathbb{N}$, and $f \in AC^n([a,b])$, then:

The left Riemann-Liouville fractional derivative of order α is defined as

$$ {}_aD_t^\alpha f(t) = \frac{1}{\Gamma(n-\alpha)} \frac{d^n}{dt^n} \int_a^t \frac{f(\tau)}{(t-\tau)^{\alpha-n+1}} d\tau, $$

$$ t \in [a,b]; $$

The right Riemann-Liouville fractional derivative of order α is defined as

$$ {}_tD_b^\alpha f(t) = (-1)^n \frac{1}{\Gamma(n-\alpha)} \frac{d^n}{dt^n} \int_t^b \frac{f(\tau)}{(\tau-t)^{\alpha-n+1}} d\tau, $$

$$ t \in [a,b]; $$

According to [25], the definition of the Riemann-Liovulle fractional derivative in the case $\alpha \in \mathbb{R}$ follows from the above given definition. In this paper, the left Riemann-Liouville fractional derivative for $\alpha \in [0, 1)$ is used, and it will be denoted by D^α throughout the text.

3. Formulation of the problem

3.1. The problem statement

In this paper, a cantilever beam of a constant geometry and made of a homogeneous isotropic viscoelastic material, carrying an arbitrary number of concentrated masses is analysed. The beam is subjected to an arbitrary transversal load and to an arbitrary transversal movement of the support. The schematic representation of the described system is presented in Fig. 1.

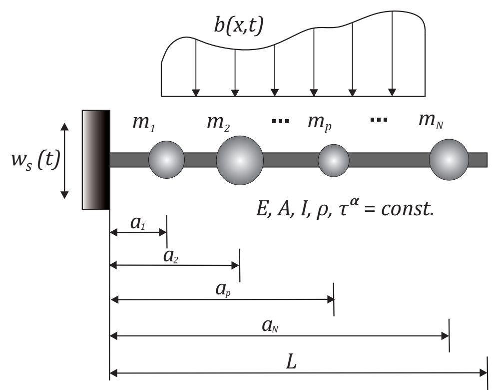

Figure 1: The schematic representation of the analysed model

Viscoelastic material behavior can be more conveniently described by using a constitutive relation with a time derivative of a fractional (non-integer) order. In this paper, the following constitutive relation is used to describe the material [21]:

$$\sigma(t) = E\left(\varepsilon(t) + \tau^\alpha D^\alpha \varepsilon(t)\right) \tag{1}$$

where $\sigma(t)$ is the normal stress, $\varepsilon(t)$ is the dilatation, E is the material elasticity modulus, and τ^α is the retardation time.

3.2. The equation of motion

For the previously described model, the derived equation of motion is of the form:

$$EIw'''' + EI\tau^\alpha D^\alpha(w'''') + \left(\rho A + \sum_{p=1}^{N} M_p \delta(x - a_p)\right)\ddot{w} = b(x,t) \tag{2}$$

where w is the transversal displacement of the beam, I is the cross-sectional moment of inertia, ρ is the material mass density, A is the cross-sectional area of the beam, x is the longitudinal coordinate, M_p is the p-th attached mass and δ is the Dirac function. In this paper, the symbol $(\bullet)'$ will be used to represent $\partial(\bullet)/\partial x$, $(\dot{\bullet})$ will symbolize $\partial(\bullet)/\partial t$, and $(\bullet)^{(\alpha)}$ will denote $D^{\alpha}(\bullet)$.

The corresponding boundary conditions were taken to be

$$w(0,t) = w_s(t) \quad \text{and} \quad w'(0,t) = EIw''(L,t) = EIw'''(L,t) = 0$$

where $w_s(t)$ is the motion function of the support. Also, the zero initial conditions were taken.

Currently, the boundary conditions are not homogeneous. In order to homogenise them, the following procedure can be applied [46]. Namely, if the beam support moves according to the function $w_s = w_s(t)$, the *absolute* transversal displacements of the beam can be decomposed into two parts - a rigid body motion of the beam, where each point moves exactly like the support, and the displacements relative to the supported end of the beam $(v(x,t))$:

$$w(x,t) = w_s(t) + v(x,t) \tag{3}$$

Introducing this relation to the equation of motion gives

$$EIv''''(x,t) + EI\tau^{\alpha}D^{\alpha}(v''''(x,t)) + \left(\rho A + \sum_{p=1}^{N} M_p\delta(x-a_p)\right)\ddot{v}(x,t) = \\ = F(x,t) \tag{4}$$

where $F(x,t) \equiv b(x,t) - \left(\rho A + \sum_{p=1}^{N} M_p\delta(x-a_p)\right)\ddot{w}_s(t)$.

This leads to the homogeneous boundary conditions:

$$v(0,t) = v'(0,t) = EIv''(L,t) = EIv'''(L,t) = 0$$

4. The Galerkin method

4.1. The system equations

Since there are concentrated masses attached to the beam along the span, the exact solution of the Eq.(4) would require the use of complex algebraic operations and complicated mode shape functions that need to satisfy the specific orthogonality conditions (e.g. [47]). The other way to find the exact solution is the multi-span beam approach, but it quickly leads to a very large number of equations with the increase of number of the attached masses. To avoid these difficulties, the approximate methods are usually suggested in literature [8], such as the Galerkin, Rayleigh-Ritz or the Finite element method. In this paper, the Galerkin method will be used to find the approximate solution of the Eq.(4).

At this point, the solution $v(x,t)$ is approximated by a series

$$v(x,t) = \sum_{i=1}^{n} \phi_i(x)q_i(t) \tag{5}$$

where n is the number of terms in the Galerkin series approximation, $\phi_i(x)$ are the trial functions for the Galerkin solution, and $q_i(t)$ are the Galerkin coefficients, herein considered to be some yet undetermined time functions. As it is known from literature [48], any function from the set of comparison functions, i.e. the functions that exactly satisfy the boundary conditions, can be used as a trial function in the Galerkin approximation. For now, it will be assumed that the trial functions $\phi_i(x)$ are known, and they will be specifically determined in the next subsection.

Taking into account the above approximation, the equation of motion becomes

$$\sum_{i=1}^{n} EI\phi_i''''(x)q_i(t) + \sum_{i=1}^{n} EI\phi_i''''(x)\tau^\alpha D^\alpha q_i(t) + \\ + \sum_{i=1}^{n} \left(\rho A + \sum_{p=1}^{N} M_p \delta(x - a_p)\right) \phi_i(x)\ddot{q}_i(t)) - F(x,t) = R^* \tag{6}$$

where $R^* \neq 0$ is a nonzero residual that arises due to the introduced approximation. The Galerkin weighted residual method requires that the integral of the weighted residual over the whole problem domain vanishes [7], while *the trial functions* are used as the weighting functions, i.e. $\int_0^L \phi_j(x)R^* dx = 0, \quad j = 1, 2, \dots, n$. This produces the following system of n equations

$$\sum_{i=1}^{n} \left(\int_0^L EI\phi_i''''(x)\phi_j(x)dx\right) q_i(t) + \sum_{i=1}^{n} \left(\int_0^L EI\tau^\alpha \phi_i''''(x)\phi_j(x)dx\right) D^\alpha q_i(t) + \\ + \sum_{i=1}^{n} \left(\int_0^L \left(\rho A + \sum_{p=1}^{N} M_p \delta(x - a_p)\right) \phi_i(x)\phi_j(x)dx\right) \ddot{q}_i(t)) = \\ = \int_0^L F(x,t)\phi_j(x)dx \equiv Q_j(t), \quad j = 1, 2, \dots, n \tag{7}$$

which can be expressed in matrix form as

$$\mathbf{Kq} + \mathbf{Cq}^{(\alpha)} + \mathbf{M\ddot{q}} = \mathbf{Q} \tag{8}$$

where $\mathbf{q}^{(\alpha)} \equiv D^\alpha \mathbf{q}$, as stated previously, and with the matrix and vector elements calculated as

$$
\begin{aligned}
K_{ij} &= \int_0^L EI\phi_i''''(x)\phi_j(x)dx = \\
&= \int_0^L EI\phi_i''(x)\phi_j''(x)dx + EI\phi_i'''(x)\phi_j(x)|_0^L - EI\phi_i''(x)\phi_j'(x)|_0^L \\
C_{ij} &= \int_0^L EI\tau^\alpha\phi_i''''(x)\phi_j(x)dx \\
&= \int_0^L EI\tau^\alpha\phi_i''(x)\phi_j''(x)dx + \tau^\alpha EI\phi_i'''(x)\phi_j(x)|_0^L - \tau^\alpha EI\phi_i''(x)\phi_j'(x)|_0^L \\
M_{ij} &= \int_0^L \left(\rho A + \sum_{p=1}^N M_p\delta(x-a_p)\right)\phi_i(x)\phi_j(x)dx \\
Q_j &= \int_0^L F(x,t)\phi_j(x)dx \\
\mathbf{q}^T &= [q_1, q_2, ..., q_n]
\end{aligned}
$$

4.2. The trial functions

In the Galerkin method, the trial functions are chosen from the set of *comparison* functions, i.e. the functions that *exactly* satisfy all the boundary conditions of the problem, and are mutually orthogonal. In this paper, the mode shape functions for the bare beam (with no concentrated masses attached) with the appropriate boundary conditions are used as the trial functions $\phi_i(x)$ [7].

Accordingly, for a cantilever beam, the trial functions are taken as:

$$
\phi_i(x) = \sqrt{\frac{1}{\rho AL}}\left(\cos\beta_i x - \cosh\beta_i x + \frac{\cos\beta_i L + \cosh\beta_i L}{\sin\beta_i L + \sinh\beta_i L}(\sin\beta_i x - \sinh\beta_i x)\right)
$$

where ${\beta_i}^4 = \bar{\omega}_i^4\frac{\rho A}{EI}$ is the $i-$th dimensionless frequency parameter of the bare beam, and $\bar{\omega}_i$ is th $i-$th natural frequency of the bare beam. The frequency parameters β_i are determined from the frequency equation

$$
\cos\beta_i L\cosh\beta_i L = -1
$$

which has an infinite number of roots, but only the first n roots are used for constructing the Galerkin trial functions.

4.3. Calculation of the matrix elements

Since the trial functions are chosen to be orthogonal and to satisfy the boundary conditions, the elements of the Galerkin system matrices can be evaluated as follows:

$$
\begin{aligned}
K_{ij} &= \int_0^L EI\phi_i''(x)\phi_j''(x)dx = \begin{cases} \int_0^L EI\left(\phi_i''(x)\right)^2 dx & \text{for } i=j \\ 0 & \text{for } i \neq j \end{cases} \\
C_{ij} &= \int_0^L EI\tau^\alpha \phi_i''(x)\phi_j(x)''dx \; = \tau^\alpha K_{ij} \\
M_{ij} &= \begin{cases} \int_0^L \rho A\phi_i^2(x)dx + \sum_{p=1}^N M_p\phi_i^2(a_p) & \text{for } i=j \\ \sum_{p=1}^N M_p\phi_i(a_p)\phi_j(a_p) & \text{for } i \neq j \end{cases} \\
Q_j &= \int_0^L F(x,t)\phi_j(x)dx
\end{aligned}
\tag{9}
$$

When Eq.(9) are introduced to Eq.(8), the differential equation obtained is equivalent to the one found in [49], if in Eq.(1) it is taken that $E \cdot \tau^\alpha = E_1$, where E_1 is defined in [49]. Also, as it can be seen, the matrix $\mathbf{M}$ is symmetric, but not diagonal, due to the presence of the attached masses. Therefore, the system of equations expressed with Eq.(8) is a non-homogeneous *coupled* system of fractional order differential equations, with n equations and n unknown time functions $q_i(t)$. This type of system of equations cannot be solved directly, due to the presence of the fractional order derivative. In this paper, in order to find the solution, the Fourier transformation is used. Moreover, first the unit impulse response of the system is determined, and then the total response for an arbitrary load and support motion function are calculated by the convolution integral of the unit impulse response and the load function.

4.4. Determining the impulse response

The impulse response of the system is called the Green function, here denoted with $G(t)$. For a unit impulse response calculation, a unite impulse load is used instead of arbitrary transversal load and inertia forces represented by $F(x,t)$, the Eq.(8) becomes

$$
\mathbf{K}\mathbf{g}(t) + \mathbf{C}\mathbf{g}^{(\alpha)}(t) + \mathbf{M}\ddot{\mathbf{g}}(t) = \boldsymbol{\delta}_m(t) \tag{10}
$$

where $\mathbf{g}^T(t) = [G_1(t), G_2(t), ..., G_n(t)]$, and $\boldsymbol{\delta}_m(t)$ is the unit impulse vector in the m-th coordinate, used in the same manner as in [44]. This means that, if n terms in the Galerkin approximation are considered, $\boldsymbol{\delta}_m(t)$ is a vector of n elements, all of which are zero, except for the m-th one, that equals the Dirac delta function, thus representing the unit impulse load in the m-th coordinate.

It should be pointed out that the equations (8) and (10) formally resemble the equation obtained in a modal analysis. However, since the trial functions $\phi_i(x)$ are the mode shape functions of a *bare beam*, they *are not* the actual mode shape functions of the analysed beam with the attached masses. Therefore, the time functions $q_i(t)$ are also not the modal coordinates, and thus in the Galerkin systems (8) and (10) the vibration modes are *coupled*. Consequently, the functions $q_i(t)$ represent the coupled *total* response functions of the system, and similarly, $G_i(t)$ are the coupled *impulse* responses of the system.

As it has already been mentioned, the Fourier transformation will be used to solve the system of equations (10). Now, when the Fourier transformation is applied to the Green functions $G_i(t)$, they become $\hat{G}_i(\omega)$. Note that for the transition from the original, real, time domain, to the Fourier, frequency domain of the Green function, one is referred to [44, 50]. Introducing the described Fourier transform, the equation (10) becomes

$$\mathbf{K}\hat{\mathbf{g}}(\omega) + (i\omega)^{\alpha}\mathbf{C}\hat{\mathbf{g}}(\omega) + (i\omega)^{2}\mathbf{M}\hat{\mathbf{g}}(\omega) = \mathbf{e}_m(\omega) \tag{11}$$

where $\mathbf{e}_m(\omega)$ is the Fourier transform of the unit impulse vector $\boldsymbol{\delta}_m(t)$. Eq.(11) can be expressed more conveniently as

$$\left[\mathbf{K} + (i\omega)^{\alpha}\mathbf{C} + (i\omega)^{2}\mathbf{M}\right]\hat{\mathbf{g}}(\omega) = \mathbf{e}_m(\omega) \qquad \text{or} \qquad \mathbf{A}(\omega)\hat{\mathbf{g}}(\omega) = \mathbf{e}_m(\omega) \tag{12}$$

where i is the imaginary unit, and $\mathbf{A}(\omega) = \mathbf{K} + (i\omega)^{\alpha}\mathbf{C} + (i\omega)^{2}\mathbf{M}$. It is obvious that the matrix $\mathbf{A}$ is not diagonal, since $\mathbf{M}$ is not diagonal.

Now, as previously noted, in Eq.(12) the vibration modes are coupled. In order to determine the natural frequencies of the system, it is necessary to decouple the modes. Moreover, the decoupled system of equations is much easier to solve.

In this paper, the case with the proportional damping is analysed. According to [49], if the proportional damping is encountered and the beam stiffness matrices depend on only one elastic modulus, then the modal projection method can be used to decouple the system of equations 12, same as in the *undamped* case. Moreover, according to [44], the *matrix of eigenvectors* of the corresponding *undamped system* can be used to diagonalize the system matrices $\mathbf{M}$, $\mathbf{K}$ and $\mathbf{C}$, if they are linearly dependant.

The eigenproblem for the corresponding undamped system can be expressed as

$$\left(\mathbf{K} - \omega_r{}^{2}\mathbf{M}\right)\mathbf{u}_r = \mathbf{0}, \qquad r = 1, 2, \ldots n \tag{13}$$

where ω_r is the $r-$th natural frequency and $\mathbf{u}_r$ is the $r-$th eigenvector of the undamped system. These eigenvectors are normalized with respect to the mass matrix $\mathbf{M}$, through which the influence of the attached concentrated masses is introduced (Eq.(9)). The eigenvectors $\mathbf{u}_r$ also satisfy the *generalized* orthogonality condition

$$\mathbf{u}_r^{\mathrm{T}}\mathbf{M}\mathbf{u}_s = \mathbf{u}_r^{\mathrm{T}}\mathbf{K}\mathbf{u}_s = 0 \qquad \text{for} \qquad r \neq s.$$

By solving the stated eigenproblem, the n eigenvectors $\mathbf{u}_r$ are obtained and they can be organized into the matrix of eigenvectors as $\mathbf{\Phi} = [\mathbf{u}_1, \mathbf{u}_2, \ldots, \mathbf{u}_n]$. As has been shown in [44], this matrix can be used to diagonalize the damped system matrices:

$$\begin{aligned}
\mathbf{M}^{\mathrm{d}} &= \mathbf{\Phi}^{\mathrm{T}}\mathbf{M}\mathbf{\Phi} = \mathbf{I} \\
\mathbf{K}^{\mathrm{d}} &= \mathbf{\Phi}^{\mathrm{T}}\mathbf{K}\mathbf{\Phi} \\
\mathbf{C}^{\mathrm{d}} &= \mathbf{\Phi}^{\mathrm{T}}\mathbf{C}\mathbf{\Phi} = \tau^{\alpha}\mathbf{K}^{\mathrm{d}} \\
&\text{or} \\
\mathbf{A}^{\mathrm{d}} &= \mathbf{\Phi}^{\mathrm{T}}\mathbf{A}\mathbf{\Phi}
\end{aligned} \tag{14}$$

where $\mathbf{M}^{\mathrm{d}}$, $\mathbf{K}^{\mathrm{d}}$, $\mathbf{C}^{\mathrm{d}}$ and $\mathbf{A}^{\mathrm{d}}$ are the diagonal mass, stiffness, damping and system matrices, respectively, τ^{α} is the retardation time and $\mathbf{I}$ is the identity matrix.

Since the matrix $\mathbf{\Phi}$ diagonalizes the system matrices, it effectively decouples the vibration modes. Therefore, it holds that: $\hat{\boldsymbol{\eta}}(\omega) = \mathbf{\Phi}^{\mathrm{T}}\hat{\mathbf{g}}(\omega)$, or, stated differently: $\hat{\mathbf{g}}(\omega) = \mathbf{\Phi}\hat{\boldsymbol{\eta}}(\omega)$, where

$$\hat{\boldsymbol{\eta}}^{T}(\omega) = [\hat{\eta}_1(\omega), \hat{\eta}_2(\omega), \ldots, \hat{\eta}_n(\omega)]$$

and $\hat{\eta}_i(\omega)$ is the Fourier transform of $\eta_i(t)$, which is the *decoupled* unit response of the system in the $i-$th vibration mode, that is, $\eta_i(t)$ is the $i-$th *generalized (modal) coordinate* of the whole system (with the attached masses).

Bearing in mind the above relations, and multiplying Eq.(12) from the left by $\mathbf{\Phi}^{\mathrm{T}}$, it becomes

$$\mathbf{A}^{\mathrm{d}}(\omega)\hat{\boldsymbol{\eta}}(\omega) = \mathbf{\Phi}^{\mathrm{T}}\mathbf{e}_m(\omega) \tag{15}$$

Eq.(15) represents the decoupled system of independent equations and it can be solved for the transformed decoupled impulse response as

$$\hat{\boldsymbol{\eta}}(\omega) = \left(\mathbf{A}^{\mathrm{d}}(\omega)\right)^{-1}\mathbf{\Phi}^{\mathrm{T}}\mathbf{e}(\omega) \quad ,$$

or

$$\hat{\eta}_r(\omega) = \frac{1}{A^d_{rr}}\sum_{s=1}^{n}\Phi_{sr}e_s \quad , \qquad r = 1, 2, \ldots, n \tag{16}$$

Taking into account equations (12) and (14), Eq.(16) can be expressed as

$$\hat{\eta}_r(\omega) = \frac{\mathbf{u}_r \cdot \mathbf{e}_m}{K^d_{rr} + (i\omega)^{\alpha}C^d_{rr} + (i\omega)^2 M^d_{rr}} = \frac{\Phi_{mr}}{K^d_{rr} + (i\omega)^{\alpha}C^d_{rr} + (i\omega)^2 M^d_{rr}} \tag{17}$$

The denominator of the above expression is the characteristic polynomial associated with Eq.(17), and the corresponding characteristic equation is:

$$K^d_{rr} + (i\omega)^{\alpha}C^d_{rr} + (i\omega)^2 M^d_{rr} = 0 \tag{18}$$

If the substitution $i\omega = s$ is introduced and minding that $C^d_{rr} = \tau^{\alpha}K^d_{rr}$, the characteristic equation can be rearranged as follows

$$s^2 + \tau^{\alpha}\omega_r^2 s^{\alpha} + \omega_r^2 = 0 \tag{19}$$

where it is taken that $\omega_r^2 = K^d_{rr}/M^d_{rr}$. It can be shown that this characteristic equation of decoupled system is equivalent to the equation corresponding to a single-mass system [51], and it has two roots - a complex conjugate pair $s_{1,2} = -\sigma_r \pm i\Omega_r$ [22]. The real part of the root $s_{1,2}$ represents the damping ratio, while the imaginery part represents the damped frequency of the system. In order to determine these roots, in general case when $\alpha \in \mathbb{R}$, the characteristic equation cannot be solved directly, and an analytical procedure involving trigonometric functions has to be applied. Namely, another substitution is introduced [22]:

$s = \xi e^{i\psi}$, which transforms the characteristic equation for the r-th vibration mode into

$$\xi_r^2 e^{2i\psi_r} + \tau^\alpha \omega_r^2 \xi_r^\alpha e^{\alpha i \psi_r} + \omega_r^2 = 0$$

Using the Euler's formula and noting that both real and imaginary parts should equal zero, the following system of trigonometric equations is obtained:

$$\begin{aligned} \xi_r^2 \cos 2\psi_r + \tau^\alpha \omega_r^2 \xi_r^\alpha \cos \alpha\psi_r + \omega_r^2 = 0 \\ \xi_r^2 \sin 2\psi_r + \tau^\alpha \omega_r^2 \xi_r^\alpha \sin \alpha\psi_r = 0 \end{aligned}$$

This system can easily be solved for the unknown parameters ξ and ψ by taking that $X_1 = \xi_r^2$ and $X_2 = \tau^\alpha \omega_r^2 \xi_r^\alpha$, then solving it for the unknown X_1 and X_2, and then calculating the sought parameters ξ and ψ. This leads to the solution

$$\begin{aligned} \xi_r &= \sqrt{\frac{K_{rr}^d}{M_{rr}^d} \frac{\sin \alpha\psi_r}{\sin (2-\alpha)\psi_r}} \\ \tau^\alpha &= -\frac{\sin 2\psi_r}{\sin (2-\alpha)\psi_r} \xi_r^{-\alpha} \end{aligned}$$

where ψ_r is related to the given retardation time τ^α by the second equation, and the given system of two equations can be solved to obtain ψ_r and ξ_r, thus defining the complex conjugate roots of the characteristic equation Eq.(19).

However, although Eq.(17) gives the transformed decoupled Green functions, the inverse Fourier transform required to determine the real Green functions is not so straightforward. But it can be shown [50] that each real decoupled Green function consists of two parts, namely

$$\eta_r(t) = K_{1r}(t) + K_{2r}(t) \tag{20}$$

The first term is the residue part, and the second one is the characteristic integral. These two terms can be calculated as

$$\begin{aligned} K_{1r}(t) &= a_{1r} e^{(-\sigma_r t)} \sin(\Omega_r t + a_{2r}) \\ K_{2r}(t) &= \frac{\tau^\alpha \omega_r^2 \sin(\pi\alpha)}{\pi} \int_0^\infty \frac{z^\alpha e^{-zt} dz}{[z^2 + \tau^\alpha \omega_r^2 z^\alpha \cos(\pi\alpha) + \omega_r^2]^2 + [\tau^\alpha \omega_r^2 z^\alpha \sin(\pi\alpha)]} \end{aligned} \tag{21}$$

where

$$\begin{aligned} a_{1r} &= \Phi_{mr} \frac{2}{\sqrt{\mu_r^2 + \nu_r^2}} \quad , \qquad a_{2r} = \arctan\left(\frac{\mu_r}{\nu_r}\right) \\ \mu_r &= \mathrm{Re}[P'(s_{1,2})] \\ \nu_r &= \mathrm{Im}[P'(s_{1,2})] \\ P(s) &= s^2 + \tau^\alpha \omega_r^2 s^\alpha + \omega_r^2 \\ P'(s) &\equiv dP(s)/ds = 2s + \alpha \tau^\alpha \omega_r^2 s^{\alpha-1} \end{aligned} \tag{22}$$

It can be shown that the drift part $K_{2r}(t)$ is numerically much smaller than $K_{1r}(t)$ and that it diminishes with time, so it can be neglected with only a slight loss in accuracy [43]. Thus it will not be considered here, leaving only the first term.

Finally, when the decoupled real Green functions are known, the coupled impulse response functions can be determined by

$$\mathbf{g}(t) = \mathbf{\Phi}\boldsymbol{\eta}(t) \quad . \tag{23}$$

4.5. The total response of the system

After the impulse system response has been determined, the total response can be calculated as a convolution of the impulse response and the actual loads, that is:

$$q_i(t) = \int_0^t G_i(t-\tau)Q_i(\tau)d\tau \tag{24}$$

where Q_i are the functions defined in Eq.(9).

When the time functions $q_i(t)$ are known, the relative transversal displacements of the beam can be calculated by Eq.(5), and the absolute beam displacements can be obtained by Eq.(3), which presents the solution to the analyzed problem.

5. Validation of the proposed approximate solution

In this Section the approximate solution proposed in this paper will be validated. However, to the best of authors' knowledge there is no exact solution to the herein analysed problem in literature. For this reason, the proposed solution will be validated for a special case whith *only one* mass attached to the tip of the beam, since in [43] Freundlich presented the exact analytical solution for this problem.

Moreover, in order to validate the applied Galerkin spatial discretisation for the case with multiple attached masses, the results will be compared to the Finite element method (FEM) solution. However, the fractional damping FEM solution would require some additional numerical approximation schemes for treating the fractional derivative (such as the application of Grünwald-Letnikov time discretisation scheme in the Newmark integration procedure, as it was done in [29] for instance). This would in turn also introduce additional numerical error as compared to the approximate solution presented in this paper, where only the spatial discretisation is used. Therefore, the presented procedure and the trial functions used will be validated for the case with classical viscous damping, i.e. for an integer order of the time derivative - $\alpha = 1.0$. The comparison of the obtained results shows that the presented model with the Galerkin discretisation and the chosen trial functions adequately describes the beam behaviour also in the case of multiple attached masses present, and that it can be successfully applied to a system with integer order damping.

5.1. The case with one mass attached - comparison with the exact solution

As previously mentioned, in [43] Freundlich presented the exact analytical solution to the problem of vibrations of a viscoelastic cantilever beam carrying a tip mass due to the transversal load and motion of the support. In that paper, the material was also defined by a fractional-order derivative constitutive equation, and the cantilevered beam was subjected to an arbitrary distributed transversal load and an arbitrary transversal support motion. However, there was only one mass attached to the tip of the beam. This led to the equation of motion of the same form as Eq.(2), only without the summation term (which represents the effect of the other attached masses). The influence of the attached tip mass was introduced via the appropriate boundary conditions, while both the mass translational and rotational inertia were considered. Accordingly, the boundary conditions at the free end ($x = L$) differed from the herein adopted homogeneous ones, and they were defined as

$$m_p \ddot{w}(L,t) = -V(L,t) \qquad \text{and} \qquad I_p(\ddot{w'})(L,t) = M_b(L,t) \tag{25}$$

where m_p and I_p are the mass and the moment of inertia of the attached tip mass, respectively, $V(L,t)$ and $M_b(L,t)$ are the transversal force and the bending moment at the free end, respectively, and $w(x,t)$ is the transversal displacement.

In order to validate the proposed approximate solution, the numerical results were obtained by setting all the parameters' values to be exactly as in [43], while only the rotational inertia of the tip mass was neglected. Therefore, the following parameter values were adopted: beam length $L = 0.8\ m$, mass density $\rho = 1190.0\ kg/m^3$, cross-sectional area $A = 5 \cdot 10^-4\ m^2$, bending stiffness $EI = 1.667 \cdot 10^-8\ m^4$ and elasticity modulus of $E = 3.2\ GPa$, attached tip mass $m_p = 0.0476\ kg$, while the order of the fractional derivative α, and retardation time τ^α were varied. The mass of the beam can be calculated as $m_b = \rho A L$, and the attached tip mass is taken to be $m_p = \mu\, m_b$, where μ is the attached mass to beam mass ratio. The motion function of the support was taken to be

$$w_s(t) = w_0 \sin\left(\varepsilon_a \cdot t^2/2\right) \tag{26}$$

where $w_0 = 0.001\ m$ is the amplitude of the support motion, and $\varepsilon_a = 10\ s^{-2}$ is the angular acceleration of the support.

For the Galerkin solution, the number of the considered terms in the approximation series directly influences the accuracy of the solution. After preliminary numerical analysis of the beam eigenfrequency in the first vibration mode, by requiring that the approximation error be less than 0.015 percent, it was shown that the approximation with $n = 7$ terms satisfies this criterion, while presenting reasonable computational requirements. Therefore, this approximation was adopted for all the following considerations.

First, the eigenfrequencies of the described system were analysed. As previously pointed out, the *elastic* (undamped) eigenfrequencies of the system can be calculated as $\omega_r = \sqrt{\frac{K^d_{rr}}{M^d_{rr}}}$. However, the *damped* frequencies and the damping ratios correspond to the imaginary and real parts of the roots of the characteristic Eq.(18), respectively. That is, if the r-th root with the positive imaginary part is expressed as $s_r = -\sigma_r + i \cdot \Omega_r$, then σ_r will represent the damping ratio in the r-th mode, and Ω_r would represent the corresponding r-th damped frequency of the system.

Table 1 and shows these damped frequencies for both the exact analytical solution calculated in accordance with [43], and the approximate solution presented in this paper. The results are shown for various different fractional derivative orders α, as well as different attached mass to beam mass ratios μ, for the first six vibration modes. As it can be seen from the tables, the results are in very good agreement - the error in frequency value for the first mode (which is the most influential one) is less then 0.012%, while the largest error occurred, as expected, in the highest considered mode and it was 1.12%.

As it has already been mentioned, the solution presented in this paper for a case with multiple attached masses will be validated against the FEM solution in the next subsection. In order to validate the FEM solution itself, the damped frequencies obtained by FEM were also compared to the exact solution. These results are also shown in Table 1. As it can be seen, the developed FEM solution is also in a reasonable agreement to the exact analytical solution, and it is therefore adopted for later validation of the proposed approximate solution for cases with multiple attached masses.

Table 1: Damped frequencies in the first six vibration modes for the cantilever carrying only a tip mass, and with $b = 0\ kN/m$; α - fractional derivative order, $\mu = m_p/m_b$, $s_r = -\sigma_r + i \cdot \Omega_r$, $r = 1, 2, \ldots n$ - root of the characteristic equation; E - Exact solution [43], G - Galerkin approximation

Ω_i		$\alpha = 0.25$			$\alpha = 0.50$			$\alpha = 1.00$				
		E [43] $[s^{-1}]$	G $[s^{-1}]$	Error [%]	E [43] $[s^{-1}]$	G $[s^{-1}]$	Error [%]	E [43] $[s^{-1}]$	G $[s^{-1}]$	Error [%]	FEM $[s^{-1}]$	Error [%]
$\mu = 0.20$	Ω_1	38.74	38.74	0.011	38.82	38.83	0.011	38.62	38.63	-0.14	38.63	-0.12
	Ω_2	270.36	270.45	0.03	272.48	272.57	0.03	259.40	259.48	0.03	259.54	0.05
	Ω_3	796.18	797.12	0.12	808.07	809.03	0.12	483.41	483.01	-0.08	483.18	-0.05
	Ω_4	1609.85	1614.29	0.28	1645.79	1650.39	0.28	-	-	-	-	-
	Ω_5	2716.68	2730.78	0.52	2797.90	2812.65	0.53	-	-	-	-	-
	Ω_6	4118.03	4154.27	0.88	4272.78	4311.13	0.90	-	-	-	-	-
$\mu = 0.50$	Ω_1	29.89	29.90	0.01	29.94	29.95	0.01	29.81	29.82	0.01	29.83	0.04
	Ω_2	250.94	251.07	0.05	252.82	252.95	0.05	242.08	242.19	0.05	242.24	0.07
	Ω_3	768.53	769.79	0.16	779.78	781.06	0.16	492.73	492.40	-0.07	492.58	-0.03
	Ω_4	1578.04	1583.65	0.36	1612.88	1618.68	0.36	-	-	-	-	-
	Ω_5	2682.25	2699.30	0.64	2761.88	2779.72	0.65	-	-	-	-	-
	Ω_6	4081.84	4124.28	1.04	4234.49	4279.39	1.06	-	-	-	-	-
$\mu = 1.00$	Ω_1	23.08	23.09	0.01	23.12	23.12	0.01	23.03	23.03	0.01	23.04	0.05
	Ω_2	241.26	241.40	0.06	243.03	243.17	0.06	233.34	233.47	0.05	233.50	0.07
	Ω_3	756.55	757.94	0.18	767.52	768.94	0.19	495.51	495.22	-0.06	495.39	-0.02
	Ω_4	1565.23	1571.31	0.39	1599.63	1605.91	0.39	-	-	-	-	-
	Ω_5	2668.96	2687.16	0.68	2747.98	2767.01	0.69	-	-	-	-	-
	Ω_6	4068.24	4113.03	1.10	4220.10	4267.49	1.12	-	-	-	-	-

Furthermore, the displacements of the free end of the cantilever relative to its support were analysed and the approximate results obtained through the herein presented procedure were compared to the exact results of the analytical solution. In Fig. 2 the relative displacements of the free end of the beam in the first 10 seconds are shown, for the cases of $\mu = 0.25$ and $\mu = 0.75$, respectively. All the results are calculated for the value of the retardation time $\tau^{\alpha} = 0.002$ and $b = 0.0\,kN/m$. As it can be seen, the results are in a very good agreement, especially for a smaller attached tip mass. The system frequencies are practically the same (beams are moving in phase), and the amplitudes differ only slightly. It is well known that the Galerkin solution accumulates error over time [8, 52–54], so the best approximation is achieved in the first several seconds of motion.

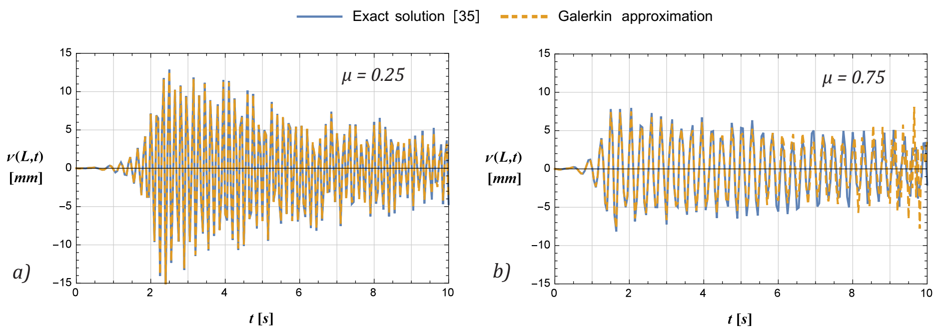

Figure 2: The relative displacements of the free end of the cantilever with only one attached mass; $\tau^{\alpha} = 0.002$, $b = 0$; dashed line - the exact solution, continuous line - the Galerkin solution; a) $\mu = 0.25$, b) $\mu = 0.75$

It should also be noted that the Galerkin solution, again, as expected, gives somewhat smaller displacements and somewhat higher frequencies than the exact solution. This is due to the fact that higher order terms in the series approximation are neglected, which could be interpreted as introducing some "additional supports" in higher vibration modes, thus increasing the stiffness of the system.

5.2. Multiple attached masses - comparison with the FEM solution

Finally, the presented Galerkin approximation was validated against the Finite Element Method (FEM) solution for a case of a cantilever beam carrying 2, 3 and 5 equidistantly attached masses of equal weight. In each considered case, total weight of the attached masses was equal to the weight of the beam. In Table 2 the system eqigenfrequencies for the first 3 modes are presented for the cases of 2,3 and 5 masses attached, for both the FEM and the proposed Galerkin solution, and the results are in very good agreement.

Aside from the frequencies, the displacements were also considered for each of the previously described cases. Fig. 3 shows the relative displacements of the free end in the first 10 seconds for the cases with 2 and 5 attached masses, and with $\alpha = 1.0$ and $\tau^{\alpha} = 0.002$. The results obtained by both methods are

Table 2: Damped frequencies for a cantilever beam carrying N masses, and with $\alpha = 1.0$, $\tau^\alpha = 0.002$ and $b = 0$; FEM - Finite Element Method solution, G = Galerkin approximation

	Ω_i	N=2			N=3			N=5		
		FEM $[s^{-1}]$	G $[s^{-1}]$	Error [%]	FEM $[s^{-1}]$	G $[s^{-1}]$	Error [%]	FEM $[s^{-1}]$	G $[s^{-1}]$	Error [%]
$\mu = 1.0$	Ω_1	28.83	28.82	-0.03	31.20	31.19	-0.03	33.30	33.29	-0.03
	Ω_2	175.46	175.50	0.03	191.26	191.37	0.06	203.74	203.84	0.05
	Ω_3	497.39	502.51	1.03	448.84	450.98	0.48	473.47	475.86	0.50

in reasonably good agreement, which implies that the presented solution is also valid for analysis of beams with multiple attached masses.

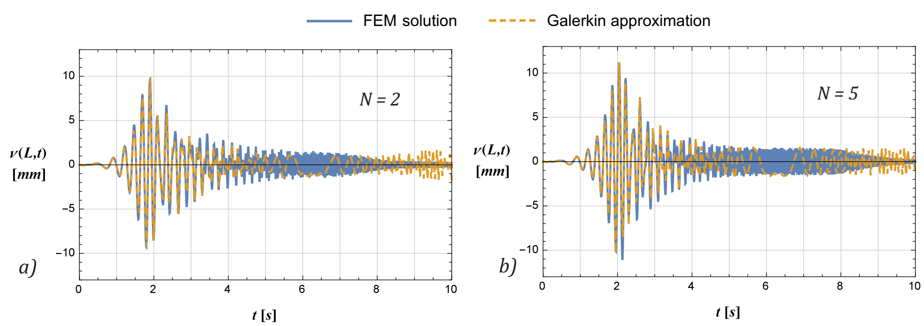

Figure 3: The relative displacements of the free end of the cantilever with $N = 2$ attached masses and $\mu = 0.5, \alpha = 1.0, \tau^\alpha = 0.002, b = 0$; continuous line - the FEM solution, dashed line - the Galerkin solution

As it can be seen, the Galerkin solution proposed in this paper gives a very good approximation in all the considered cases, for beams carrying one or more attached masses, with various fractional derivative orders and attached masses weights. Therefore, it can be concluded that the solution proposed in this paper does present a valid approximate solution to the stated problem. In further text, the proposed solution will be used for further numerical analysis of forced vibrations of a beam carrying multiple attached masses.

6. Numerical analysis

In this section, the numerical analysis of forced vibrations of a viscoelastic cantilever beam due to the motion of the support is presented. The fixed end of the beam moves as described by the function $w_s(t)$ defined in the previous Section, with the same parameter values adopted. Parameters describing the order of the fractional derivative, retardation time, and the number, weight and position of the attached masses were varied, and the results are presented in the following text.

6.1. Frequency analysis

Influence of the fractional derivative order and the retardation time

First, the influence of the order of the fractional derivative α and the time of retardation τ^α on the damped frequencies and damping ratios of the beam is analysed. Since the first vibration mode is the most influential one, the effects on the first damped frequency were of most interest. As already pointed out, the real part σ_r of the complex roots of the characteristic equation represents the damping ratio, while the imaginary part Ω_r represents the damped frequency. In Fig. 4 both these characteristics for the first vibration mode are shown for several different fractional derivative orders. Each point of the presented diagram was obtained by choosing the appropriate value for α, and letting τ^α range from 0 to ∞. If the trigonometric functions are used in solution, as described in Section 4, since $\tau^\alpha = -\frac{\sin 2\psi}{\sin(2-\alpha)\psi}\xi_r^{-\alpha}$, the angle ψ ranges from $\pi/2$ to $\pi/(2-\alpha)$. The diagram is in complete agreement with the used fractional Kelvin-Voigt model and diagrams given in [22]. However, on the given diagram, the shortcomings of the fractional Kelvin-Voigt model become apparent. Namely, for relatively low fractional derivative order, cca. $\alpha < 0.6$, frequencies of the beam appear to be increasing with the increase of the retardation time (therefore also the damping ratio), which makes no physical sense. However, there are systems and cases were this model is applicable and where it produces valid results, as has been discussed in several papers, e.g. [22], especially for somewhat higher order of the fractional derivative.

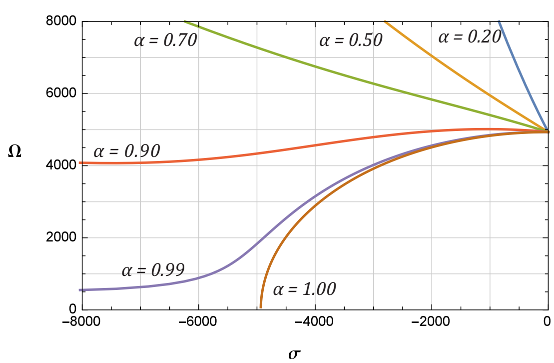

Figure 4: The influence of the order of the fractional derivative on the complex root of the characteristic equation in the first vibration mode

Influence of the number and weight of the attached masses

Next, the influence of the number of the attached masses N and their weight, represented by the attached mass to beam mass ratio μ, is considered. For this analysis, the fractional derivative order and time of retardation were kept constant, at values of $\alpha = 0.5$ and $\tau^\alpha = 0.002$. Five models were considered - a bear beam with no attached masses, and beams with 1, 2, 3 and 4 attached masses. Each attached mass was of equal mass m_p, which was calculated as

$m_p = \mu\, \rho AL$, while the ratio μ was varied between the limits of 0 and 1. The results are presented in Fig. 5 and Fig. 6, showing the dependence of the damping ratio σ_1 and the damped frequency of the beam Ω_1, respectively, on the number of the attached masses N and the ratio μ. It can be seen from these two diagrams that more attached masses reduce the beam frequency, as expected, and they also reduce the damping effects, monotonically and proportionally.

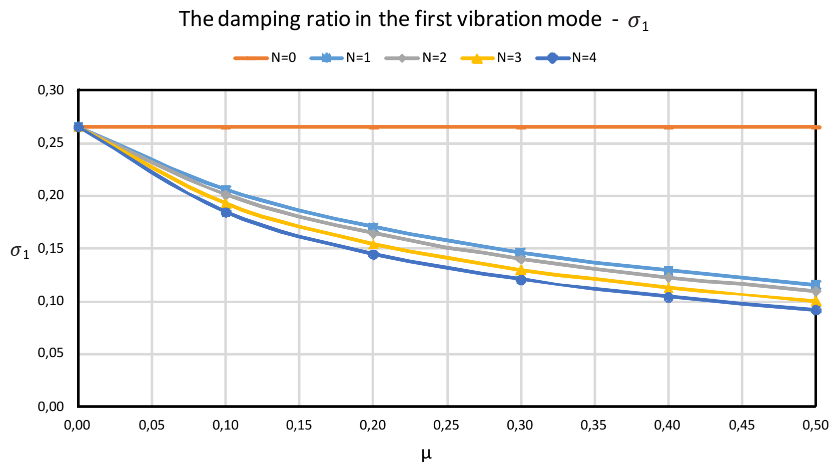

Figure 5: The influence of the number and weight of the attached masses on the damping ratio σ_1 in the first vibration mode

Influence of the position of the attached mass

Finally, the influence of the position of the attached masses on the damping ratios and the damped frequencies of the beam was analysed. As in the previous analysis, the order of the fractional derivative and the retardation time were kept constant, at the values of $\alpha = 0.5$ and $\tau^\alpha = 0.002$. For the present analysis, the case with two attached masses was considered. One of the masses was always attached at the free and, while the other was "slid" along the beam, and the influence of these various positions of the attached masses was analysed. The "slid" mass was calculated as $m_p = \mu_p \rho AL$ and it was positioned at a_p, while the tip mass was always positioned at the free end of the beam at $a_e = L$ and it was determined as $m_e = \mu_e \rho AL$. For the present analysis, the weights of the attached masses were chosen as $\mu_e = 0.5$, while the weight ratio for the "slid" mass was varied, and it was taken to be 0.25, 0.50, and 1.00, successively. The results are presented in Fig. 7 and Fig. 8, where the influence on the damping ratio σ_1 and the damped frequency Ω_1 are shown, respectively.

6.2. Displacement analysis

In further analysis, the displacements of the free end of the cantilever beam relative to the clamped end were considered. The time of retardation was kept

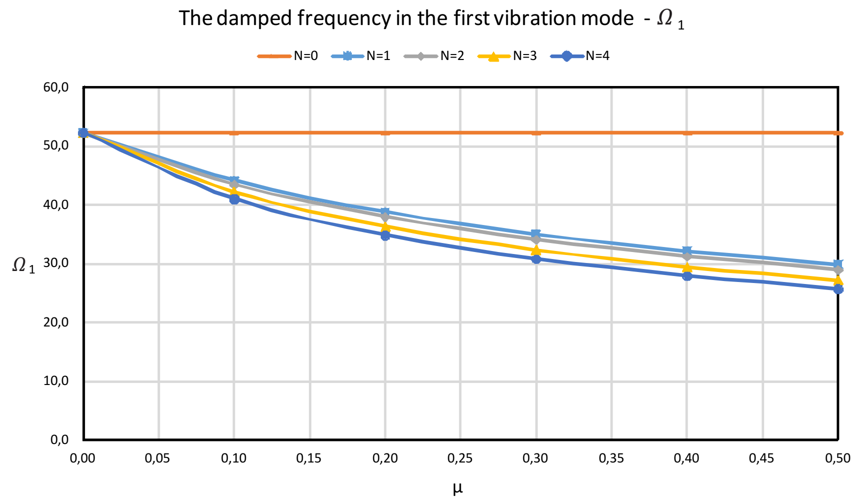

Figure 6: The influence of the number and weight of the attached masses on the damped frequency of the beam Ω_1 in the first vibration mode

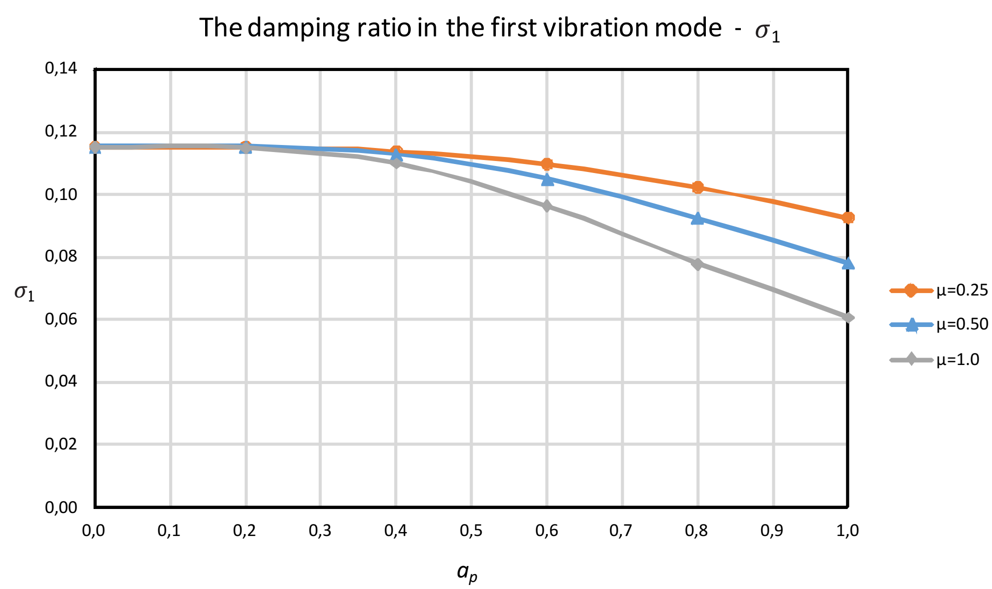

Figure 7: The influence of the position and weight of the attached masses on the damping ratio σ_1 in the first vibration mode

constant throughout the analysis and it was fixed at $\tau^\alpha = 0.002$. Other parameters were varied according to each tested influence.

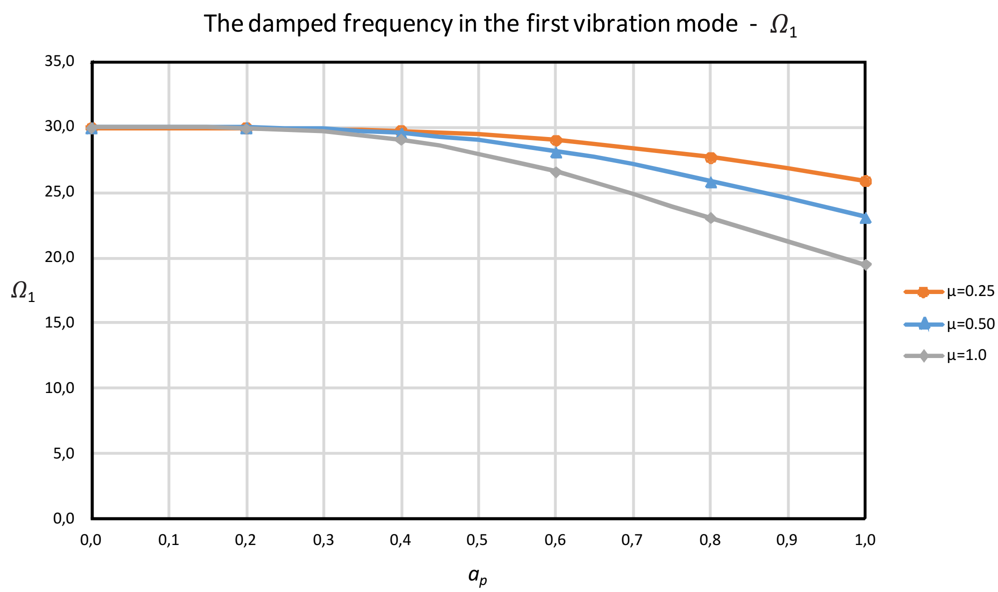

Figure 8: The influence of the position and weight of the attached masses on the damped frequency of the beam Ω_1 in the first vibration mode

Influence of the order of the fractional derivative

For the analysis of influence of the fractional derivative order α on the total beam response, represented by the relative displacements of the free end $v(L,t)$, the case with 4 equidistant attached masses of equal weight was considered. Each of the attached masses was taken to be $m_p = 0.5\rho AL$. The results are presented in Fig. 9, which shows the relative displacements $v(L,t)$ in the first 10 seconds of motion. The diagram clearly shows that the increase in the fractional derivative order leads to a higher damping effect, while the frequency of the total beam response remains practically unaffected.

Influence of the number of the attached masses

The influence of the number of the attached masses on the total beam response was also analysed. In each analysed model, the fractional derivative order was kept fixed at $\alpha = 0.5$, and masses were equidistantly positioned. The number of the attached masses was varied, but they were always of mutually equal weight, and the total weight of the attached masses was always equal to the weight of the bare beam, that is: $\mu = 1.0/N$ and $m_p = \mu\, m_b,\ p = 1, 2, \ldots, N$. Four cases were considered - a bear beam, and a beam carrying 1, 3, and 5 attached masses, i.e. $N \in \{0, 1, 3, 5\}$. The obtained relative displacements of the free end of the beam $v(L,t)$ in the first 10 seconds of motion are presented in Fig. 10, for the cases of 0, 1, 3 and 5 attached masses, respectively. It can be observed that the more mass is concentrated at the tip of the cantilever, both

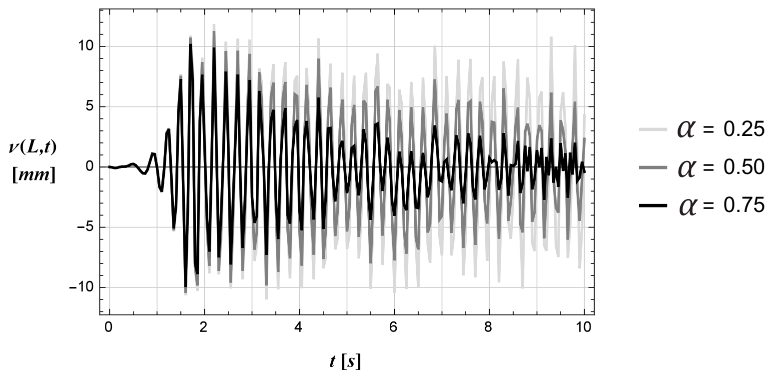

Figure 9: Relative displacements of the free end of the beam for different order of the fractional derivative

the vibration amplitudes and frequency of the beam decrease more. There is also a resonance region shift observable. The first resonance occurs between 2 and 3 seconds of motion, depending on the considered case.

It should also be pointed out that, under the stated analysis conditions, the more masses are attached to the beam, the more that system resembles the case of the bare beam of two times bigger mass. It is as if the attached mass (that is kept equal to the original weight of the bare beam in each considered case) gets "smeared" along the beam, and theoretically, for a case with $N \to \infty$, the original beam with N attached masses would practically be the same as a beam of twice the original beam's mass.

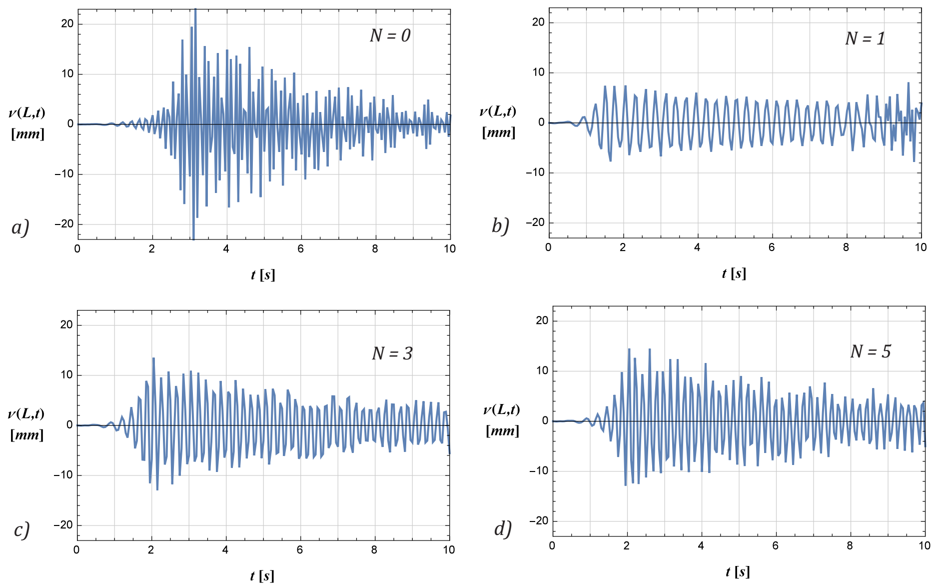

Figure 10: Relative displacements of the free end of the beam with different number of the attached masses; a) $N = 0$, b) $N = 1$, c) $N = 3$, d) $N = 5$

Influence of the weight of the attached masses

For the analysis of the influence of the weight of the attached masses, a case of a beam with $N = 4$ equidistant attached masses of equal weight was considered. Each mass was taken to be $m_p = \mu \rho A L$, while the ratio μ was varied. Four different cases were considered, that is: $\mu \in \{0.0, 0.10, 0.25, 0.50\}$. The relative displacements of the free end of the beam in the first 10 seconds of motion are presented in Fig. 11. It can be seen that the heavier masses are attached, the lower the response frequency and vibration amplitudes. Moreover, as the attached weight increases, the damping influence becomes less distinct (the motion amplitudes decay slower), since because of the considerable weight of the attached masses (for instance, for the case of $\mu = 0.50$, the total attached mass is 2 times greater than the mass of the bare beam), it is harder for the beam to attenuate the movement of the attached masses.

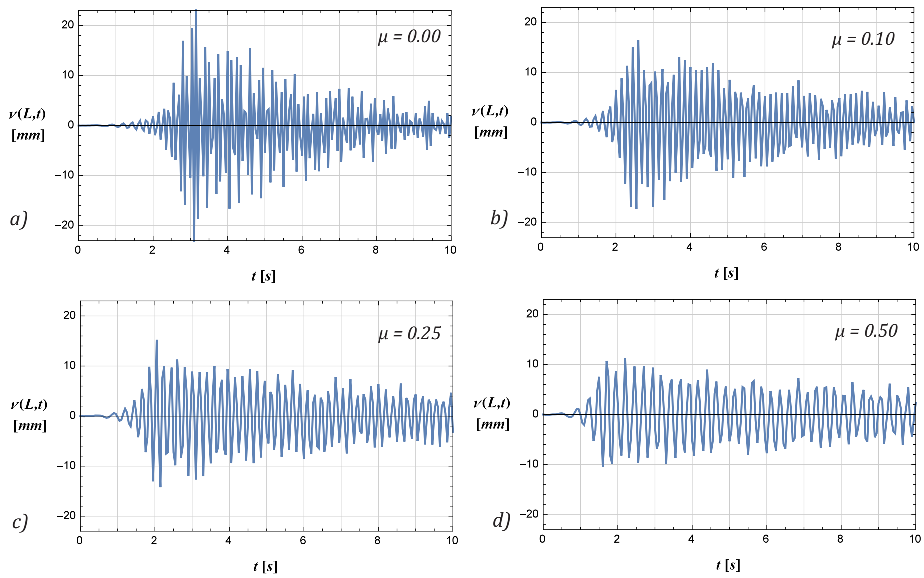

Figure 11: Relative displacements of the free end of the beam due to various weight of the 4 equidistantly attached masses; $\alpha = 0.5$, $N = 4$; a) $\mu = 0.00$, b) $\mu = 0.10$, c) $\mu = 0.25$, d) $\mu = 0.50$

Influence of the position of the attached masses

Finally, the influence of the attached mass position on the total response of the beam was also analysed. For this purpose, a model with $N = 2$ attached masses was considered, with the same characteristics as for the frequency and damping ratio analysis - one of the attached masses of $m_e = 0.5\,\rho AL$ was always kept at the free end of the beam, while the other mass of the same weight, i.e. $m_p = 0.5\,\rho AL$ was "slid" along the beam, that is, the various positions of the "sliding" attached mass were considered. The position of the "sliding" mass is represented by the parameter a_p, and 6 different positions were analysed: $a_p \in \{0.00, 0.33, 0.66, 1.0\}$. Material parameters were held constant at $\alpha = 0.5$ and $\tau^\alpha = 0.002$. The results are summarised in Fig. 12, where the relative displacements of the free end over the first 10 seconds of motion are presented. It can be seen that the closer the "sliding" mass gets to the free end of the beam, the lower the response frequency and vibration amplitudes.

It can also be observed that the position of the "sliding" mass influences the dynamical characteristics of the beam by shifting the resonance region. Namely, the first resonance region is around 2 seconds for all the analysed models, but in the case of the "sliding" attached mass positioned near the midspan of the beam, as well as right at the free end of the beam, the second resonance occurs somewhat sooner, after slightly less than 10 seconds of motion. The second resonance region occurs in viscoelastic models described by fractional order derivative constitutive equation, as presented in [43], for instance.

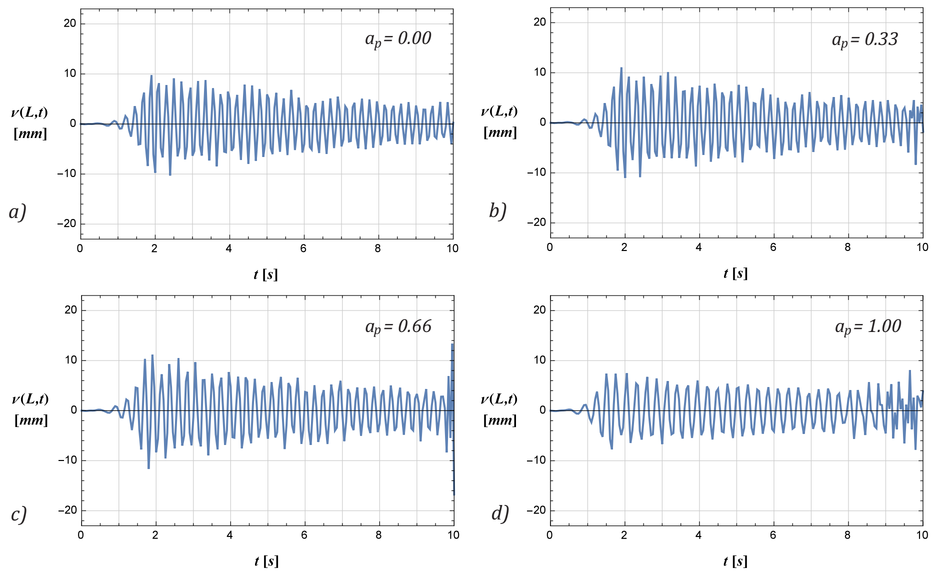

Figure 12: Relative displacements of the free end of the beam for different position of the two attached masses; $\alpha = 0.5$, $N = 2$; a) $a_p = 0.00$, b) $a_p = 0.33$, c) $a_p = 0.66$, d) $a_p = 1.00$

7. Concluding remarks

In this paper, vibrations of a viscoelastic cantilever beam carrying an arbitrary number of attached concentrated masses and exposed to an arbitrary transversal motion of the support was analysed. The constitutive relation was formulated with the use of fractional order Kelvin-Voigt model, and the equations of motion were derived accordingly. These equations were solved by using the Galerkin approximation method, combined with the Fourier integral transform method and residue theory. The proposed solution was validated against the exact analytical solution for a special case of a beam carrying only a tip mass that was presented in [43], as well as against the FEM solution for a case of a beam carrying multiple masses, but with an integer order time derivative, instead of the fractional order derivative that was ultimately aimed for by the solution proposed in this paper. All the tested results were in good agreement, so the proposed solution is indeed a novel and valid approximate solution to the analysed problem.

The proposed method presents an approximate solution to a general problem of transient vibration of a cantilever beam carrying an arbitrary number of attached masses, while also providing the possibility to use different values of fractional parameters. Its application was demonstrated in numerical analyses of dependence of dynamic characteristics such as eigenfrequencies and damping ratios of the beam, on several parameters such as the number, weight and position of the attached masses, as well as on the fractional parameters, i.e. the order of the fractional derivative and the retardation time.

The presented solution should be extended to an even more general case of a Timoshenko beam and other higher order beam theories, or by introducing material and/or geometrical non-linearities or the non-local effects, or by including some attached stiffness elements. Moreover, the exact analytical solution for the problem solved in this paper should be further sought and found.

Acknowledgements

The authors would like to thank Professor Jan Freundlich from the Faculty of Automotive and Construction Machinery Engineering, Warsaw University of Technology, for providing the material that was very helpful in completing the validation study.

This research was supported by the Ministry of Education, Science and Technology of the Republic of Serbia, through the Mathematical Institute of SASA, Belgrade, and the Grant No. 174001.

The author D. Karličić was supported by the Marie Skłodowska-Curie Actions - European Commission fellowship: 799201-METACTIVE.

References

[1] XD Xie, Nan Wu, Ka Veng Yuen, and Quan Wang. Energy harvesting from high-rise buildings by a piezoelectric coupled cantilever with a proof mass. *International Journal of Engineering Science*, 72:98–106, 2013.

[2] Xinlei Fu and Wei-Hsin Liao. Nondimensional model and parametric studies of impact piezoelectric energy harvesting with dissipation. *Journal of Sound and Vibration*, 429:78–95, 2018.

[3] Yu Chen. On the vibration of beams or rods carrying a concentrated mass. *Journal of Applied Mechanics*, 30(2):310–311, 1963.

[4] KH Low. On the methods to derive frequency equations of beams carrying multiple masses. *International Journal of Mechanical Sciences*, 43(3):871–881, 2001.

[5] Giuseppe Failla and Adolfo Santini. On euler–bernoulli discontinuous beam solutions via uniform-beam green's functions. *International Journal of Solids and Structures*, 44(22-23):7666–7687, 2007.

[6] Giuseppe Failla, Francesco Paolo Pinnola, and Gioacchino Alotta. Exact frequency response of bars with multiple dampers. *Acta Mechanica*, 228 (1):49–68, 2017.

[7] Leonard Meirovitch. *Principles and techniques of vibrations*, volume 1. Prentice Hall New Jersey, 1997.

[8] MN Hamdan and L Abdel Latif. On the numerical convergence of discretization methods for the free vibrations of beams with attached inertia elements. *Journal of sound and vibration*, 169(4):527–545, 1994.

[9] J-S Wu and T-L Lin. Free vibration analysis of a uniform cantilever beam with point masses by an analytical-and-numerical-combined method. *Journal of Sound and Vibration*, 136(2):201–213, 1990.

[10] J-S Wu and D-W Chen. Dynamic analysis of a uniform cantilever beam carrying a number of elastically mounted point masses with dampers. *Journal of Sound and Vibration*, 229(3):549–578, 2000.

[11] MA Eltaher, MA Agwa, and FF Mahmoud. Nanobeam sensor for measuring a zeptogram mass. *International Journal of Mechanics and Materials in Design*, 12(2):211–221, 2016.

[12] M Ghommem and A Abdelkefi. Nonlinear reduced-order modeling and effectiveness of electrically-actuated microbeams for bio-mass sensing applications. *International Journal of Mechanics and Materials in Design*, pages 1–19.

[13] HR Ali-Akbari, S Ceballes, and A Abdelkefi. Nonlinear performance analysis of forced carbon nanotube-based bio-mass sensors. *International Journal of Mechanics and Materials in Design*, pages 1–25, 2018.

[14] Zhi-Bin Shen, Li-Ping Sheng, Xian-Fang Li, and Guo-Jin Tang. Nonlocal timoshenko beam theory for vibration of carbon nanotube-based biosensor. *Physica E: Low-Dimensional Systems and Nanostructures*, 44(7-8):1169–1175, 2012.

[15] Keivan Kiani. A meshless approach for free transverse vibration of embedded single-walled nanotubes with arbitrary boundary conditions accounting for nonlocal effect. *International Journal of Mechanical Sciences*, 52(10): 1343–1356, 2010.

[16] Keivan Kiani, Hamed Ghaffari, and Bahman Mehri. Application of elastically supported single-walled carbon nanotubes for sensing arbitrarily attached nano-objects. *Current Applied Physics*, 13(1):107–120, 2013.

[17] Sondipon Adhikari. *Damping models for structural vibration*. PhD thesis, University of Cambridge, 2001.

[18] Yongjun Lei, Michael Ian Friswell, and Sondipon Adhikari. A galerkin method for distributed systems with non-local damping. *International Journal of Solids and Structures*, 43(11-12):3381–3400, 2006.

[19] MI Friswell, S Adhikari, and Y Lei. Vibration analysis of beams with nonlocal foundations using the finite element method. *International Journal for Numerical Methods in Engineering*, 71(11):1365–1386, 2007.

[20] RC Koeller. Applications of fractional calculus to the theory of viscoelasticity. *Journal of Applied Mechanics*, 51(2):299–307, 1984.

[21] Yuriy A Rossikhin. Reflections on two parallel ways in the progress of fractional calculus in mechanics of solids. *Applied Mechanics Reviews*, 63 (1):010701, 2010.

[22] Yuriy A Rossikhin and Marina V Shitikova. Application of fractional calculus for dynamic problems of solid mechanics: novel trends and recent results. *Applied Mechanics Reviews*, 63(1):010801, 2010.

[23] Katica R Hedrih-Stevanović and Aleksandar Filipovski. Longitudinal creep vibrations of a fractional derivative order rheological rod with variable cross section. *Facta universitatis-series: Mechanics, Automatic Control and Robotics*, 3(12):327–349, 2002.

[24] Katica Stevanovic Hedrih. The transversal creeping vibrations of a fractional derivative order constitutive relation of nonhomogeneous beam. *Mathematical Problems in Engineering*, 2006, 2006. DOI:10.1155/MPE/2006/46236.

[25] Teodor M Atanackovic, Stevan Pilipovic, Bogoljub Stankovic, and Dusan Zorica. *Fractional calculus with applications in mechanics: wave propagation, impact and variational principles.* John Wiley & Sons, 2014.

[26] Mikael Enelund and B Lennart Josefson. Time-domain finite element analysis of viscoelastic structures with fractional derivatives constitutive relations. *AIAA journal*, 35(10):1630–1637, 1997.

[27] Ana Cristina Galucio, J-F Deü, and Roger Ohayon. Finite element formulation of viscoelastic sandwich beams using fractional derivative operators. *Computational Mechanics*, 33(4):282–291, 2004.

[28] Salvatore Di Lorenzo, Mario Di Paola, Francesco P Pinnola, and Antonina Pirrotta. Stochastic response of fractionally damped beams. *Probabilistic Engineering Mechanics*, 35:37–43, 2014.

[29] Christian Bucher and Antonina Pirrotta. Dynamic finite element analysis of fractionally damped structural systems in the time domain. *Acta Mechanica*, 226(12):3977–3990, 2015.

[30] R Ansari, M Faraji Oskouie, F Sadeghi, and M Bazdid-Vahdati. Free vibration of fractional viscoelastic timoshenko nanobeams using the nonlocal elasticity theory. *Physica E: Low-dimensional Systems and Nanostructures*, 74:318–327, 2015.

[31] Ronald L Bagley and RA Calico. Fractional order state equations for the control of viscoelasticallydamped structures. *Journal of Guidance, Control, and Dynamics*, 14(2):304–311, 1991.

[32] Francesco Paolo Pinnola. Statistical correlation of fractional oscillator response by complex spectral moments and state variable expansion. *Communications in Nonlinear Science and Numerical Simulation*, 39:343–359, 2016.

[33] Pol D Spanos and Giovanni Malara. Nonlinear random vibrations of beams with fractional derivative elements. *Journal of Engineering Mechanics*, 140 (9):04014069, 2014.

[34] Wojciech Sumelka, Tomasz Blaszczyk, and Christian Liebold. Fractional euler–bernoulli beams: Theory, numerical study and experimental validation. *European Journal of Mechanics-A/Solids*, 54:243–251, 2015.

[35] K Alsaif and MA Foda. Vibration suppression of a beam structure by intermediate masses and springs. *Journal of Sound and Vibration*, 256(4): 629–645, 2002.

[36] Mario Di Paola and G Fileccia Scimemi. Finite element method on fractional visco-elastic frames. *Computers & Structures*, 164:15–22, 2016.

[37] Milan Cajić, Danilo Karličić, and Mihailo Lazarević. Nonlocal vibration of a fractional order viscoelastic nanobeam with attached nanoparticle. *Theoretical and Applied Mechanics*, 42(3):167–190, 2015.

[38] Milan Cajić, Mihailo Lazarević, Danilo Karličić, HongGuang Sun, and Xiaoting Liu. Fractional-order model for the vibration of a nanobeam influenced by an axial magnetic field and attached nanoparticles. *Acta Mechanica*, 229(12):4791–4815, 2018.

[39] Masoud Rezaei, Siamak E Khadem, and Peyman Firoozy. Broadband and tunable pzt energy harvesting utilizing local nonlinearity and tip mass effects. *International Journal of Engineering Science*, 118:1–15, 2017.

[40] M Eissa and YA Amer. Vibration control of a cantilever beam subject to both external and parametric excitation. *Applied mathematics and computation*, 152(3):611–619, 2004.

[41] Paweł Łabędzki, Rafał Pawlikowski, and Andrzej Radowicz. Transverse vibration of a cantilever beam under base excitation using fractional rheological model. In *AIP Conference Proceedings*, volume 2029, page 020034. AIP Publishing, 2018.

[42] Jan Freundlich. Vibrations of a simply supported beam with a fractional viscoelastic material model–supports movement excitation. *Shock and Vibration*, 20(6):1103–1112, 2013.

[43] Jan Freundlich. Transient vibrations of a fractional kelvin-voigt viscoelastic cantilever beam with a tip mass and subjected to a base excitation. *Journal of Sound and Vibration*, 438:99–115, 2019.

[44] Ingo Schäfer and Siegmar Kempfle. Impulse responses of fractional damped systems. *Nonlinear Dynamics*, 38(1-4):61–68, 2004.

[45] Ngan Tran, Mergen H Ghayesh, and Maziar Arjomandi. Ambient vibration energy harvesters: A review on nonlinear techniques for performance enhancement. *International Journal of Engineering Science*, 127:162–185, 2018.

[46] Peter Hagedorn and Anirvan DasGupta. *Vibrations and waves in continuous mechanical systems.* John Wiley & Sons, 2007.

[47] Giuseppe Failla. An exact modal analysis approach to vibration analysis of structures with mass-spring subsystems and rotational joints. *Journal of Sound and Vibration*, 438:191–219, 2019.

[48] Singiresu S Rao. *Vibration of continuous systems*, volume 464. Wiley Online Library, 2007.

[49] M Giovagnoni and G Berti. A fractional derivative model for single-link mechanism vibration. *Meccanica*, 27(2):131–138, 1992.

[50] Siegmar Kempfle, Ingo Schäfer, and Horst Beyer. Fractional calculus via functional calculus: theory and applications. *Nonlinear Dynamics*, 29(1-4): 99–127, 2002.

[51] Yu A Rossikhin and MV Shitikova. Application of fractional derivatives to the analysis of damped vibrations of viscoelastic single mass systems. *Acta Mechanica*, 120(1-4):109–125, 1997.

[52] Saumya Bajpai and Ambit K Pany. A priori error estimates of fully discrete finite element galerkin method for kelvin-voigt viscoelastic fluid flow model. *arXiv preprint arXiv:1903.00975*, 2019.

[53] Leonard Meirovitch. *Elements of vibration analysis.* McGraw-Hill Science, Engineering & Mathematics, 1975.

[54] MN Hamdan and BA Jubran. Free and forced vibrations of a restrained uniform beam carrying an intermediate lumped mass and a rotary inertia. *Journal of Sound and Vibration*, 150(2):203–216, 1991.